Peptides 34 (2012) 26–38

Contents lists available at SciVerse ScienceDirect

Peptides

journal homepage: www.elsevier.com/locate/peptides

Peptide fingerprinting of the neurotoxic fractions isolated from the secretions of sea anemones *Stichodactyla helianthus* and *Bunodosoma granulifera*. New members of the APETx-like family identified by a 454 pyrosequencing approach

Armando Alexei Rodríguez[a], Juliana Silva Cassoli[b], Fei Sa[c], Zhi Qiang Dong[c], José Carlos de Freitas[d], Adriano M.C. Pimenta[b], Maria Elena de Lima[b], Katsuhiro Konno[e], Simon Ming Yuen Lee[c], Anoland Garateix[a], André J. Zaharenko[f,*]

[a] *Centro de Bioproductos Marinos (Cebimar), Loma y 37, Nuevo Vedado, Habana 10400, Cuba*
[b] *Laboratório de Venenos e Toxinas Animais, Universidade Federal de Minas Gerais (UFMG), Belo Horizonte, MG, Brazil*
[c] *State Key Laboratory of Quality Research in Chinese Medicine, Institute of Chinese Medical Sciences, University of Macau, Macao, China*
[d] *Instituto de Biociências, Depto. de Fisiologia, Universidade de São Paulo, São Paulo, Brazil*
[e] *Institute of Natural Medicine, University of Toyama, Toyama, Japan*
[f] *Laboratório de Genética, Instituto Butantan, Avenida Vital Brazil, 1500, CEP 05503-900 São Paulo, Brazil*

ARTICLE INFO

Article history:
Received 21 August 2011
Received in revised form 5 October 2011
Accepted 5 October 2011
Available online 12 October 2011

Keywords:
Sea anemone
Peptide fingerprint
Peptidomics
Venom
Toxin
Transcriptomics
454 sequencing
Stichodactyla helianthus
Bunodosoma granulifera

ABSTRACT

Sea anemones are known to contain a wide diversity of biologically active peptides, mostly unexplored according to recent peptidomic and transcriptomic studies. In the present work, the neurotoxic fractions from the exudates of *Stichodactyla helianthus* and *Bunodosoma granulifera* were analyzed by reversed-phase chromatography and mass spectrometry. The first peptide fingerprints of these sea anemones were assessed, revealing the largest number of peptide components (156) so far found in sea anemone species, as well as the richer peptide diversity of *B. granulifera* in relation to *S. helianthus*. The transcriptomic analysis of *B. granulifera*, performed by massive cDNA sequencing with 454 pyrosequencing approach allowed the discovery of five new APETx-like peptides (U-AITX-Bg1a–e – including the full sequences of their precursors for four of them), which together with type 1 sea anemone sodium channel toxins constitute a very distinguishable feature of studied sea anemone species belonging to genus *Bunodosoma*. The molecular modeling of these new APETx-like peptides showed a distribution of positively charged and aromatic residues in putative contact surfaces as observed in other animal toxins. On the other hand, they also showed variable electrostatic potentials, thus suggesting a docking onto their targeted channels in different spatial orientations. Moreover several crab paralyzing toxins (other than U-AITX-Bg1a–e), which induce a variety of symptoms in crabs, were isolated. Some of them presumably belong to new classes of crab-paralyzing peptide toxins, especially those with molecular masses below 2 kDa, which represent the smallest peptide toxins found in sea anemones.

1. Introduction

Animal venoms are sources of biologically active peptides, mainly ion channels toxins. So far several hundreds of peptide sequences have been reported from some of the most studied venomous organisms such as scorpions, snakes, cone snails and spiders [44]. The strategies employed for the discovery of these peptide toxins have generally involved bioassay-guided chromatographic purifications followed by chemical and pharmacological characterizations. More recently peptidomic/proteomic and genomic (transcriptomic) approaches have converged into venomics to accomplish whole venom analyses that speed up the finding of new peptides and proteins of taxonomical and pharmacological interest [11,12,17,20,28,31,34,50,51,53,57,61,62,67,69,79,81,82,85], through the combination of advanced liquid chromatography, mass spectrometry and molecular biology techniques. On the other hand, the history of venom analyses in sea anemones is just starting, hitherto comprising only two reports [45,85]. After 40 years of bioassay-guided purifications of sea anemones peptide toxins, the first peptidomic analysis of a sea anemone (*Bunodosoma cangicum*) [85] was reported, allowing the detection of 81 components including 9 novel peptides. Subsequently, 43 novel sequences were discovered by the transcriptomic analysis of *Anemonia viridis* (formerly *Anemonia sulcata*) [45]. These two

* Corresponding author. Tel.: +55 11 3726 7222x2141.
E-mail addresses: armando@cebimar.cu, aara259@gmail.com (A.A. Rodríguez), a.j.zaharenko@ig.com.br, zaharenko@usp.br (A.J. Zaharenko).

0196-9781/$ – see front matter © 2011 Elsevier Inc. All rights reserved.
doi:10.1016/j.peptides.2011.10.011

recent studies, together with the long history of bioassay-guided purifications, account for about a total of 150 peptide sequences so far discovered from less than 35 sea anemone species, which have been barely explored since the peptide diversity contained in sea anemones species is highly superior [45,85] to the number of toxins currently discovered from them. Therefore, in addition to the known ion channel toxins, protease inhibitors and cytolytic peptides isolated from sea anemones, many other families of peptides with novel structures and biological targets await being discovered and characterized [63].

Stichodactyla helianthus (family Stichodactylidae, genus *Stichodactyla*) and *Bunodosoma granulifera* (family Actiniidae, genus *Bunodosoma*) are among the previously studied sea anemones. However, few toxins have been isolated either from whole extracts or from mucus [2,14,21,32,43,47,72], and there are no reports describing in greater detail the peptide diversity present in the neurotoxic fractions of these species. For such purpose, it has been previously shown the suitability of starting from the sea anemone mucus since it is rich in toxic components, and does not contain animal body contaminants [85], in contrast to whole body extracts. The previous peptidomic report employed sea anemone venom extracted by electrical stimulation of specimens in isolated marine environment [85]. Another mucus extraction methodology is based on immersion of the animals in distilled water [30,43,72], producing a sea salt-free sample without requiring any electrical equipment. However this methodology has not been combined with peptidomic studies of sea anemones.

In the present work, the mucuses of *S. helianthus* and *B. granulifera* were obtained by immersion of live specimens in distilled water. The resulting samples were fractionated in Sephadex G-50 to isolate their respective neurotoxic pools, which were submitted to reversed-phase chromatography. The resulting fractions were analyzed by mass spectrometry and tested for their toxicity to crabs. Peptide diversities were described in terms of molecular mass and hydrophobicity, and compared with previous results obtained from *B. cangicum* [85]. Moreover, a transcriptomic analysis of *B. granulifera* based on cDNA sequencing by the 454 GS Junior pyrosequencing system revealed the existence of new APETx-like peptides; some of them were identified among the isolated peptides. Several reversed-phase fractions inducing a variety of toxicity symptoms on crabs were found, some of them presumably belonging to new classes of toxins.

2. Materials and methods

2.1. Extraction of sea anemone secretion and chromatographic procedure

Ten *B. granulifera* specimens and two *S. helianthus* specimens were collected at the northeast coast of Havana, Cuba, and carried to the laboratory. All specimens of the same species were immersed in 500 mL distilled water during 10 min to extract the secreted mucus, according to a previous report [72]. Both exudates were lyophilized, dissolved in 0.1 M ammonium acetate, and centrifuged at 2000 × *g* during 30 min to remove cloudiness. Then, the samples were fractionated by gel filtration chromatography using a Sephadex G-50 column of dimensions 1.9 cm × 131 cm (Amersham Biosciences, Uppsala, Sweden), as previously described by Lagos et al. [46]. The respective neurotoxic fractions of *B. granulifera* and *S. helianthus* were defined within the same elution volumes as Bcg-III (2–5 kDa approximately), the neurotoxic fraction of *B. cangicum* venom, previously obtained from a similar Sephadex G-50 column [46]. The neurotoxic fractions from *B. granulifera* and *S. helianthus* were submitted to reversed-phase HPLC in an ÄKTA Purifier system (Amersham Biosciences, Uppsala, Sweden) using a semi-preparative column, CAPCELL PAK C-18, 10 mm × 250 mm (Shiseido Corp., Kyoto, Japan). The HPLC conditions used were: 0.1% trifluoroacetic acid (TFA) in water (solvent A) and acetonitrile containing 0.1% TFA (solvent B). The chromatographic runs were performed at a flow rate of 2.5 mL/min using a 10–60% gradient of solvent B over 40 min, after an isocratic step using 10% ACN during 2.25 min. UV detection was monitored at 214 and 280 nm. Each of the individual sub-fractions from Fr 3-4 were manually collected and lyophilized or concentrated for further molecular mass assessments by MALDI-TOF mass spectrometry. Most intense fractions were re-purified in an analytical column (CAPCELL PAK C-18, 4.6 mm × 150 mm i.d.), using a slower gradient of 0.5%B/min to achieve better resolution.

The retention of a peptide expressed as percentage of acetonitrile (%ACN) was estimated from the formulas $\%ACN = 100\phi$ and $\phi_e = \phi_0 + (\Delta\phi/t_G)\cdot(t_R - t_0 - t_D)$ [78], therefore $\%ACN_e = \%ACN_0 + (\Delta\%ACN/t_G)\cdot(t_R - t_0 - t_D)$, being t_R the retention time of compound X; t_0 the elution time of a non-retained compound (6 min), t_D the equipment dwell time (0.25 min), $\Delta\%ACN/t_G$ the gradient slope (50%/40 min = 1.25%/min), $\%ACN_e$ the percentage of acetonitrile at elution of compound X, $\%ACN_0$ percentage of acetonitrile at the gradient start (10%). Then, $\%ACN_e = 10\% + 1.25\%/\text{min}\cdot(t_R - 6.25\ \text{min})$. Considering the previous isocratic step, at 10% ACN during 2.25 min, $t_{delay} = 2.25$ min is introduced in the calculation so $\%ACN_e = 10\% + 1.25\%/\text{min}\cdot(t_R - 8.50\ \text{min})$.

The proteinaceous contents of the secretions and neurotoxic fractions were estimated by the bicinchoninic acid (BCA) method [77] following the manufacturer's instructions (Pierce, Rockford, IL, USA).

2.2. Mass spectrometry analyses

Reversed-phase chromatographic fractions were submitted to mass spectrometric analyses, which were carried out using an AutoFlex III MALDI-TOF/TOF mass spectrometer (Bruker Daltonics, Billerica, USA), controlled by the FlexControl 3.0 software (Bruker Daltonics, Billerica, USA). The samples were mixed with two different matrixes (i) α-cyano-4-hydroxycinnamic acid matrix solution (1:2, v/v) and (ii) super-2-hydroxy-5-methoxybenzoic acid (s-DHB) (1:2, v/v) directly into a MTP AnchorChip 600/384 MALDI target plates (Bruker Daltonics, Billerica, USA) and dried at room temperature. Protein average masses (5000–20,000 Da) were obtained in linear mode with external calibration, using the Protein Calibration Standard (Bruker Daltonics, Billerica, USA). The peptide monoisotopic masses (900–5000 Da) were obtained in reflector mode with external calibration, using the Peptide Calibration Standard (Bruker Daltonics, Billerica, USA). The mass spectrometric data analyses were performed using the software FlexAnalysis 3.0 (Bruker Daltonics, Billerica, USA).

Software GPMAW 9.0 (Lighthouse Data, Denmark) [66] was used for the theoretical calculations of molecular masses. Sea anemone peptide sequences used for calculation of molecular masses of known toxins were extracted from [63]. Venom maps were constructed by using Microsoft Excel 2007 (Microsoft, USA). The histograms were constructed with the statistical software Origin 6.0 (Microcal Software, MA, USA).

2.3. Transcriptomic analysis

2.3.1. RNA extraction, reverse transcription and 454 pyrosequencing

Based on the results obtained in the molecular masses measurements of the peptides, as well as the higher abundance of toxins in *B. granulifera*, we decided to focus our analysis only on the transcriptomics of this species. The total RNA was extracted

from tentacles tissues of *B. granulifera* specimens using the TRIZOL® reagent (Invitrogen, Carlsbad, CA) according to the manufacturer's instructions. DNA digestion was performed using DNase I (Sigma, St. Louis, MO). After DNase I treatment, total RNA was purified using RNeasy Mini Spin Column (Qiagen). The quality and quantity of the total RNA were detected using RNA 6000 pico LabChip® kit in Agilent 2100 bioanalyzer. Also, the total RNA quantity was measured using Quant-iT™ RNA BR Assay Kit in Qubit® 2.0 Fluorometer. cDNA was synthesized using Roche double-stranded cDNA synthesis kit (Roche Applied Sciences, USA) from total RNA with oligo (dT) 20 primer. A cDNA library was prepared using cDNA rapid library preparation method kit (Roche Applied Science, GS Junior Titanium Series, USA) according to manufacturer's instruction. Approximately 500 ng of DNA was fractionated into smaller fragments (300–500 base pairs) that are subsequently polished (blunted) and subjected to adaptor ligation. The optimal amount of cDNA was adjusted to single DNA copy per bead for emulsion PCR (emPCR). Finally, the sequencing was performed in the GS Junior pyrosequencing system (Roche 454 Life Sciences, Branford, CT, USA).

2.3.2. Sequence assembly and bioinformatics

EST reads were assembled to contigs by using GS Junior Assembler software. Contigs were mapped to the NCBI non-redundant databases using MAQ (v0.7.1) [49].

2.4. Sequence similarity search and molecular modeling

The following softwares were used in the present work: FASTA, http://www.ebi.ac.uk/Tools/sss/fasta/ [65] for identifying related sequences retrieved from UniProt Knowledgebase; Clustalw2.1, http://www.ebi.ac.uk/Tools/clustalw2/index.html [48] for multiple sequence alignment of new peptides and related sequences; Jalview, http://www.jalview.org/ [83] for illustrating conserved amino acid; I-TASSER, http://zhanglab.ccmb.med.umich.edu/I-TASSER/ [70,87] for peptide molecular modeling and structure prediction; Deep View Swiss-pdb Viewer 4.0.1, http://www.expasy.org/spdbv/ [33] for viewing and calculation of electrostactic potentials of the peptide structures and models and PyMol (The PyMOL Molecular Graphics System, Version 1.2, 254 Schrödinger, LLC., http://www.pymol.org/) for viewing the structures and models. The structures of APETx1 (PDB ID: 1WQK) and APETx2 (PDB ID: 1WXN) were downloaded from the Protein Data Bank. APETx1 structure (PDB ID: 1WQK) was used as a template by I-TASSER software for the molecular modeling of the toxins. The estimated accuracy of the models were evaluated by I-TASSER software, and were validated by the tools Anolea, DFire, QMEAN, Gromos, Promotif and ProCheck, available in the "structure assessment" tool of the SWISS-MODEL structure homology-modeling server (http://swissmodel.expasy.org/workspace/) [3–5,40,42,56,88]. All the graphic designs represented were rendered by PovRay (version 3.6 by Persistence of Vision Raytracer, Pty., Ltd.).

2.5. Crab bioassay

The reversed-phase chromatographic fractions were assayed on male shore crabs *Uca thayeri* weighing 2–4 g, based on the well know crab bioassay used for detection of sea anemone neurotoxins [7,76]. Samples were injected (10 μL/g crab weight) into the base of the third walking leg. A dose of 2 μg/g crab weight (2000 μg/kg) was assayed for toxicity screening and 6 crabs were used per sample. The toxicity was considered positive when the crabs placed upward were unable to right themselves within two hours after toxin administration. Furthermore, symptoms evoked by toxin administration were carefully observed.

3. Results

3.1. Extraction of sea anemone mucus. Separation of the neurotoxic fractions

The immersion of *S. helianthus* in distilled water yielded 178 mg (average: 89 mg/specimen) whereas *B. granulifera* specimens yielded 203 mg of total proteinaceous content (average: 20.3 mg/specimen). Both exudates were submitted to gel filtration chromatography in Sephadex G-50 (Fig. 1A and B). The chromatographic profile of *B. granulifera* exudate comprised 6 main fractions (Fig. 1B) and it was very similar to the Sephadex G-50 profile of *B. cangicum*, despite these exudates were obtained from different sea anemones by using different extraction protocols. The neurotoxic fractions of *S. helianthus* and *B. granulifera* were named as Sh-3-4 and Bg-3-4, respectively. The neurotoxic fraction of *S. helianthus* (Sh-3-4) yielded 15 mg of peptide content (8.4% of the total proteinaceous content), and *B. granulifera* (Bg-3-4) 30 mg (14.8%).

3.2. Reversed-phase HPLC and mass spectrometry analyses

The reversed-phase and mass spectrometry data allowed the construction of peptide fingerprints of *S. helianthus* and *B. granulifera*, in terms of hydrophobicity and molecular mass. Additionally, the data obtained from a previous similar study of *B. cangicum* [85] was used for comparison with the sea anemones species involved in the present study. Aiming to facilitate the comparison among reversed-phase fractions, those were named similarly to the previous work [85]. Thus in the present study, the reversed-phase fractions were named as Sh or Bg (abbreviation of *S. helianthus* and *B. granulifera*) followed by a number representing the retention time (shown in Table 1). For example, Bg 6.11 is the RPC18 fraction from *B. granulifera*, eluted at 6.11 min.

The neurotoxic fractions (Sh-3-4 and Bg-3-4) were submitted to reversed-phase-C18 high performance liquid chromatography. Thirty six fractions were collected from the *S. helianthus* neurotoxic pool Sh-3-4 (Fig. 2A); most peptides eluted within a narrow range of retention times in reversed-phase chromatography, approximately 17–27 min (20–33% acetonitrile). A total of 113 peptide components were found (Table 1, Fig. 3A), ranging from 1275.9 Da to 8615.5 Da, with the highest frequency between 1500 and 2000 Da (Fig. 3D). On the other hand *B. granulifera* (Bg-3-4) yielded 53 fractions from a more complex reversed-phase profile (Fig. 2B), exhibiting a richer elution pattern in relation to *S. helianthus*, in the range 10–35 min (12–42% acetonitrile). The *B. granulifera* neurotoxic fraction (Table 2, Fig. 3E) also yielded a larger number of peptide components (156), with molecular masses from 1221.6 Da to 6983.1 Da, but more frequently within the range of 4500–5000 Da (Fig. 3E). *B. granulifera* and *B. cangicum* [85], which belong to the same genus, share a similar complexity regarding their reversed-phase profiles (Fig. 2B and C), being the group of highly abundant and hydrophobic 4–5 kDa peptides with t_R > 25 min (>32% acetonitrile) their most distinguishable feature. However, only 81 different molecular masses were found in *B. cangicum*, 78 of them above 1000 Da; with the highest occurrence within the range of 4500–5000 Da (Fig. 3F), similarly to *B. granulifera*, mainly due to the last eluting intense peaks mentioned above. On the contrary, such cluster of abundant and hydrophobic 4–5 kDa peptides is absent in *S. helianthus*.

A common feature of these sea anemone species is the presence of a notable peptide population in the range of 1.5–2 kDa (Fig. 3D–F). In both *Bunodosoma* species these peptides are present

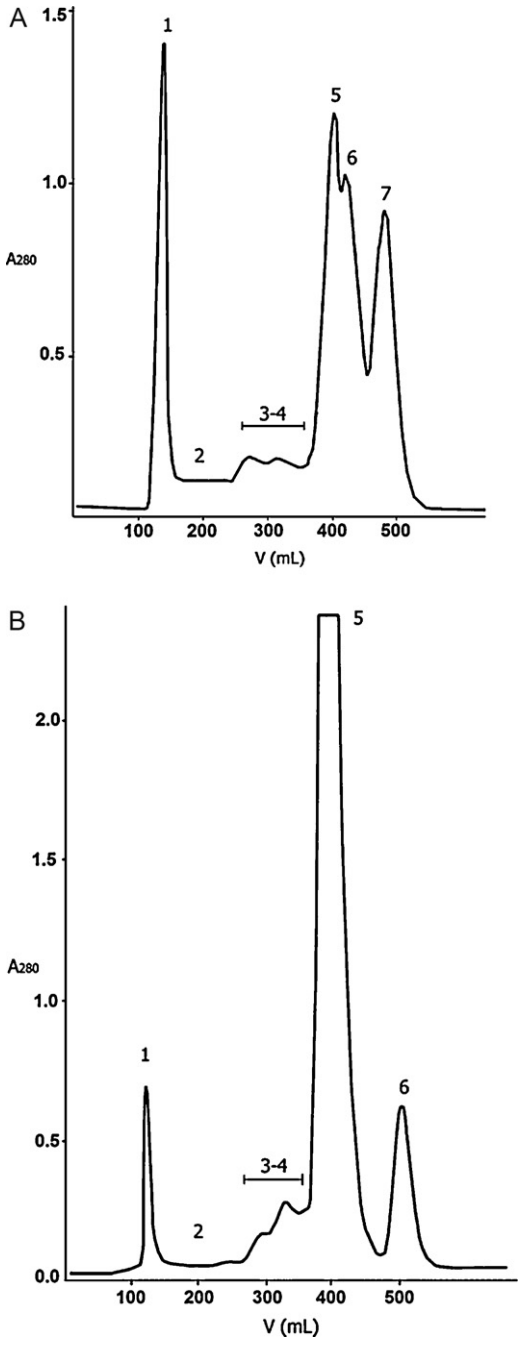

Fig. 1. Gel filtration profiles of the sea anemone exudates. Every sample (110 mg) was dissolved in 17 mL of 0.1 M ammonium acetate and applied onto a Sephadex G-50 column (1.9 cm × 131 cm). The separations were run at a flow rate of 1.7 mL/min in 0.1 M ammonium acetate; volume per fraction, 12 mL. (A) Fractionation of *Stichodactyla helianthus* exudate and (B) fractionation of *Bunodosoma granulifera* exudate.

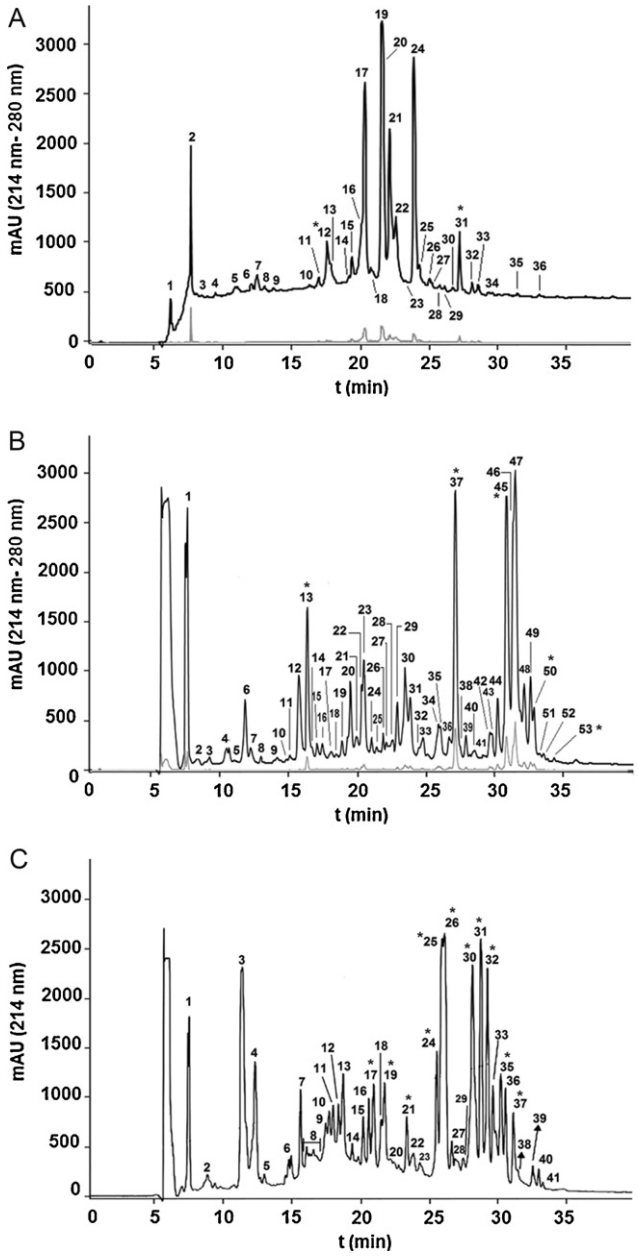

Fig. 2. Reversed-phase C18 HPLC profiles of pools 3–4 from gel filtration chromatography. Every sample (0.6–1 mg) was dissolved in 0.1% TFA and injected into a CAPCELL PAK C-18, 10 mm × 250 mm HPLC column (Shiseido Corp., Kyoto, Japan). Solvents (A) 0.1% TFA/water; (B) 0.1% TFA/acetonitrile. The separations were performed at a flow rate of 2.5 mL/min using a 10–60% gradient of solvent B over 40 min. Fractions containing known toxins and the new APETx-like peptides are marked with asterisk (see Table 1). (A) *Stichodactyla helianthus*: 12 (protease inhibitor ShPI-2 [22]) and 31 (type 2 sodium channel toxin ShI [43]). (B) *Bunodosoma granulifera*: 13 (type 1 potassium channel toxin BgK [14]); 37 (type 1 sodium channel toxins BgII and BgIII [52]); and 45, 50 and 53 (APETx-like peptides U-AITX-Bg1a, U-AITX-Bg1b and U-AITX-Bg1d, respectively); (C) *Bunodosoma cangicum*: 17, 19 and 21 (structurally novel peptides Bcg 21.00, Bcg 21.75 and Bcg 23.41 [85], respectively); 24, 31, 32 and 37 (APETx-like peptides Bcg 25.52, Bcg 28.78, Bcg 29.21 and Bcg 31.16 [85], respectively); and 25, 26, 30 and 35 (type 1 sodium channel toxins Bcg 25.96, CGTX-II [84], Bcg 28.19, Bcg 30.24 [85], respectively).

among the early eluting fractions (Fig. 3B and C), whereas in *S. helianthus* they can be found scattered throughout the reversed-phase profile (Fig. 3A).

Known sea anemone peptides isolated from *S. helianthus* and *B. granulifera* were identified by comparing their molecular masses with our experimental values. Thus ShI (5136.8 Da) [43] was located in fraction Sh 27.26 (5139.1 Da), ShPI-2 (6197.0 Da) [22] in fraction Sh 17.55 (6196.2 Da), BgII (5071.6 Da) and BgIII (5072.6 Da) [52] in fractions Bg 26.91a (5068.9 Da) and Bg 26.91b (5071.9 Da), respectively, and BgK (4275.9 Da) [2,18] in fraction Bg 16.07a (4275.8 Da). ShK (4054.8 Da) [14] and ShPI-1 (6109.9 Da) [22] could not be identified among the reversed-phase fractions.

Unlike other venomous animals [19,27,29], not a single sea anemone neurotoxin has been found in two or more species even belonging to the same genus. In the previous peptidomic study of a sea anemone, the peptides Bcg 25.96 (*B. cangicum*)

Table 1
Peptide fingerprint data of the neurotoxic pool Sh-3-4 from *Stichodactyla helianthus*.

RPC18 sample	Retention time (min)	%ACN	Toxicity	Derived fractions	$[M+H]^+$
1	6.11	<10	–	◦	1336.6; 1393.7; **1478.7**; 1606.7; 1694.7
2	7.46	<10	–	◦	**1478.7**; **1606.7**
3	8.32	<10	–	◦	1831.9; 2422.0
4	9.31	11.0	–	◦	1549.7; **1606.7**; 1779.7
5	10.90	13.0	–	◦	1584.0; 1815.3; 2027.2; 2138.0
6	12.01	14.4	–	◦	2621.6
7	12.38	14.9	–	◦	1929.1
8	13.00	15.6	–	◦	ND
9	13.61	16.4	–	◦	ND
10	16.32	19.8	–	◦	2427.7; 2566.6; 2796.9; 2977.5; 2995.5
11	16.93	20.5	–	◦	ND
12	17.55	21.3	–	◦	1384.9; 1827.9. 2387.1; 2652.2; **3342.2**; 6197.2*
13	17.79	21.6	–	◦	1630.7; 2481.7; 2551.2; **3342.2**; 3436.9; 3899.2; 4489.3
14	19.02	23.2	–	◦	2568.8; 3028.6; 3116.1; **3156.0**; **3342.2**; **5385.1**
15	19.39	23.6	–	◦	1728; 1903; **3156.0**
16	19.96	24.3	–	◦	ND
17	20.13	24.5	–	◦	3587.8; 3633.7; 5391.5
18	20.74	25.3	–	◦	1275.9; 1455.8; 1670.9; 2072.0; 2577.3; 4690.3; 4992.8; 5156.2; **5385.1**; 6143.5
19	21.48	26.2	+	a b	**3726.6** **3054.6**; **3726.6**
20	21.61	26.4	+	a b	1988.2; 2146.2; **3726.6** 2037.6; 2367.5; **3054.6**; 3681.6
21	22.05	26.9	–	◦	3097.5; 3325.4; 3803.2; 4700.6
22	22.54	27.6	–	◦	3593.4; 5394.5
23	23.20	28.4	–	◦	3453.9; 4684.2; 5297.2; 6128.2; 6214.4
24	23.89	29.2	–	◦	3371.8; **3491.2**
25	24.31	29.8	–	◦	2499.9; **3491.2**; 3585.9; 4900.1; 5474.9; 6243.1; 6832.7
26	25.05	30.7	+	◦	1879.1; **3489.3**; 3533.3; **5157.1**; 6249.4
27	25.30	31.0	–	◦	1717.9; 1788.9; 1964.0; 2448.0; 3488.3; 3530.1; 4949.1; **5157.1**; 6138.0
28	25.79	31.6	–	◦	2414.7; 3060.9; **3489.3**; 5063.5; **5329.9**
29	26.16	32.1	–	◦	1745.6; 4998.3; **5329.9**; 5491.4; 5554.8
30	26.77	32.8	++	◦	2057.9; 4871.2; 5073.2; 5153.2
31	27.26	33.5	++	◦	5140.1*
32	28.12	34.5	++	◦	5171.3
33	28.62	35.2	–	◦	7975.4; 8075.4; 8615.5
34	29.35	36.1	–	◦	1379.8; 3986.2; 6826.5; 7956.2
35	31.32	38.5	–	◦	4582.2
36	33.04	40.7	–	◦	1277.3; 1482.2

(+) Paralyzing; (++) lethal, at the dose of 2000 μg/kg; averaged masses are represented in bold type; mass values corresponding to high intensity signals are underlined; ND, not determined. Closely related masses (differences of less than 0.01%) were averaged when they appeared in adjacent fractions. The *m/z* values corresponding to molecular masses of previously reported toxins and new peptides found in our study are marked with asterisk: *m/z* 6197.2 from Sh 17.55 (protease inhibitor ShPI-2 [22]), *m/z* 5140.1 from Sh 27.26 (type 2 sodium channel toxin ShI [43]), *m/z* 4276.8 from Bg 16.07a (type 1 potassium channel toxin BgK [14]), *m/z* 5069.9 from Bg 26.91a, *m/z* 5072.9 from Bg 26.91b (type 1 sodium channel toxins BgII and BgIII [52], respectively), *m/z* 4593.5 from Bg 30.66b (U-AITX-Bg1a), *m/z* 4589.0 from Bg 32.67 (U-AITX-Bg1b), and *m/z* 4685.1 from Bg 34.22 (U-AITX-Bg1d).

and BcIII (*Bunodosoma caissarum*) exhibited identical reversed-phase chromatographic behavior and molecular masses, but it still remains to be confirmed whether these two peptides are the same toxin. In the present work we found a total of 269 peptides, most of them presumably new. Nonetheless we found some closely related fractions regarding retention times and molecular masses, not only within *Bunodosoma* but also between *Bunodosoma* and *Stichodactyla*. Some examples are Bg 16.42 (1517.7 Da) and Bcg 16.00–17.00 (1517.6 Da), Bg 25.63 (3059.3 Da) and Sh 25.79 (3059.9 Da), Bg 20.79 (3932.7 Da) and Bcg 20.64 (3933.5 Da), Bg 30.00 (4370.6 Da) and Bcg 31.16 (4371.1 Da), Bg 28.95 (4669.2 Da) and Bcg 28.78 (4669.1 Da), Bg 22.66 (4700.8 Da) and Sh 22.05 (4699.6 Da), Bg 27.35 (5071.9 Da) and Sh 26.77 (5072.2 Da).

3.3. Transcriptomic analysis

Considering the diversity of peptides with the mass range of 4000–5000 Da in the final portion of the RPC18 chromatogram of *B. granulifera* neurotoxic fraction (Bg-3-4), and the higher abundance of mass signals in this species, we decided to focus our transcriptome analysis on these proteins. Transcriptome profiling with cDNA new generation sequencing technology was used to identify some of the expressed genes of *B. granulifera*. The mRNA was isolated for the preparation of a library and subsequent pyrosequencing analysis. The total number of tags per library was approximately 59,000, with average read length of about 292 bp, which assembled 1.603 contigs. The contigs were mapped to the NCBI non-redundant databases. A preliminary data mining could reveal five matches with annotated genes encoding novel peptide toxins from the sea anemone *B. granulifera*, having from 317 to 524 bp. The full coding sequences (CDS) were obtained for four out of the five matches, including the complete translated sequences of the precursors and mature regions for neurotoxins within the mass range of 4–5 kDa (mature products), as shown in Fig. 4A and B.

Translation of the nucleotides retrieved could reveal sequence similarity to other known sea anemone toxins. A sequence similarity search (http://www.ebi.ac.uk/Tools/sss/fasta/) indicated that these peptides share homology with type 3 potassium channel toxins APETx1 [24], BDS-I and BDS-II [26], APETx2, an ASICs inhibitor [23] and the APETx-like toxins Bcg 25.52, Bcg 28.78, Bcg 29.21, Bcg 31.16 [85], BcIV [64] and BcV (accession number P86470). The highest sequence identity (57–65%) of the new toxins was observed in relation to APETx1 or APETx-like peptides. Moreover, multiple sequence alignment (http://www.ebi.ac.uk/Tools/msa/clustalw2/) showed that these new toxins are structurally close to each other (Fig. 4A), and therefore can be considered as new members of the APETx-like peptide group [64,85]. Given than their molecular targets are still unknown, these peptides (mature region, Fig. 4A) were

Table 2
Peptide fingerprint data of the neurotoxic pool Bg-3-4 from *Bunodosoma granulifera*.

RPC18 sample	Retention time (min)	%ACN	Toxicity	Derived fractions	[M+H]$^+$
1	7.23	<10	–	◦	ND
2	8.00	<10	–	◦	ND
3	8.86	10.5	–	◦	1681.6; **1819.9**
4	10.15	12.1	+	◦	**1665.5**; **1819.9**
5	10.75	12.8	–	◦	1662.2; **1665.5**; **1819.9**
6	11.52	13.8	+	◦	1730.6; 1798.0; 1817.6; 1890.7
7	11.95	14.3	+	◦	**1886.8**
8	12.73	15.3	+	◦	**1886.8**
9	13.93	16.8	–	◦	**1481.0**; **1610.0**; 1737.5; 1807.7
10	14.49	17.5	–	◦	1739.2; 1810.3; 1922.4; 2251.4
11	14.79	17.9	–	◦	1344.6; **1481.0**; **1610.0**; **1828.2**; **2037.0**; 2347.7
12	15.44	18.7	–	a b	1587.7; **1680.8**; **1726.2**; **1828.2**; **2037.0** 1687.7; **2037.0**; 2865.3; 2935.4; 3135.5
13	16.07	19.5	–	a b	**2038.2**; 4276.8* 1589.3; 1633; **1680.8**; **1726.2**; **1828.2**; **2038.2**; 2194.8
14	16.42	19.9	–	◦	**1518.7**; **2038.2**; 5461
15	16.76	20.3	–	◦	1403.7; **1518.7**; 2157.9; 2536.9; 2733.4; 2848.0
16	17.15	20.8	–	◦	ND
17	17.74	21.6	–	◦	ND
18	18.13	22.0	–	◦	2489.8; 2849.0; 3741.2; 4011.4; 4394.7; 4739.2; 4792.0
19	18.56	22.6	–	◦	4741.3; 4955.2
20	19.25	23.4	++	a b	2653.1; 2791.2; **2848.3**; 3498.1; **4775.3** **2848.3**; **4775.3**
21	19.68	24.0	++		1221.6; 2634.5; 3204.0; 3509.1; **4645.9**; 4760.6; 5848.2; 5929.5; 6067.6; 6790.5
22	19.94	24.3	+		**3188.8**; 3906.6; **4645.9**; **4745.4**
23	20.19	24.6	++		3117; **3188.8**; **4745.4**
24	20.79	25.4	++		**3188.8**; 3218.2; 3518.5; 3740.4; 3933.7; 4599.2; **4745.4**
25	21.14	25.8	–		**2634.8**; 2849.0; 3065.3; 3365.5; 4601.2; 4727.6; 5369.0
26	21.57	26.3	+		**2634.8**; 2733.9; 2833.8; 3555.8; 3605.9; 4541.9
27	21.82	26.7	++		2509.6; 2832.8; 3758.2; 4376.3; 4724.8
28	22.34	27.3	+		4745.0; 5352.6; **5373.2**
29	22.66	27.7	–	a b	2622.3; 3576.2; 3590.2; 4749.5; 4805.8; **5373.2** 4701.8; 5363.1
30	23.20	28.4	+	a b	3074.7; 3310.7; 3321.6; 4709.9 4670.7
31	23.57	28.8	–		4722.2
32	24.12	29.5	++		1249.5; 3058.6; **4797.7**; 6885.6
33	24.55	30.1	++		3173.0; **4797.7**; 6983.1
34	25.63	31.4	–		3060.3; **4598.4**; 4694.8
35	25.86	31.7	–		ND
36	26.42	32.4	++	◦	4505.8; 4541.7; **4598.4**; 4662.6; 5091.9
37	26.91	33.0	++	a b	5069.9* 5072.9*
38	27.35	33.6	–		4467.7; 4544.8; **4598.4**; 5072.9
39	27.68	34.0	–		4667.5
40	28.28	34.7	–		4189.2; 4459.6; **4598.4**
41	28.95	35.6	–		3174.3; 4216.8; 4670.2; **4736.7**; 4966.4; 5312.9; 5418.9
42	29.38	36.1	–		4214.2; **4736.7**; 4948.3
43	29.63	36.4	–		**4736.7**; 4949.3
44	30.00	36.9	–	a b	**4318.6**; **4371.6** **4318.6**; **4371.6**
45	30.66	37.7	–	a b	**4354.9** **4354.9**; 4593.5*
46	31.18	38.4	–	a b c d	**4325.6** **4354.9** 4220.3; **4325.6** 4225.8; **4354.9**
47	31.35	38.6	–	a b c	**4325.6**; 4523.4 **4325.6**; **4582.6** **4582.6**
48	31.95	39.3	–	a b c	**4386.2** **4386.2**; **4526.8** 4257.1; **4386.2**; **4526.8**
49	32.47	40.0	–	a b	**4346.2** **4346.2**
50	32.67	40.2	–	◦	4492.0; 4589.0*
51	33.17	40.8	–	◦	4323.5; 4382.9; 4525.4; **4582.6**; 4755.9; 4815.5
52	33.43	41.2	–	◦	ND
53	34.22	42.2	–	◦	4597.1; 4685.1*

(+) Paralyzing; (++) lethal, at the dose of 2000 μg/kg; averaged masses are represented in bold type; mass values corresponding to high intensity signals are underlined; ND, not determined. Closely related masses (differences of less than 0.01%) were averaged when they appeared in adjacent fractions. The *m*/*z* values corresponding to molecular masses of previously reported toxins and new peptides found in our study are marked with asterisk: *m*/*z* 6197.2 from Sh 17.55 (protease inhibitor ShPI-2 [22]), *m*/*z* 5140.1 from Sh 27.26 (type 2 sodium channel toxin Shl [43]), *m*/*z* 4276.8 from Bg 16.07a (type 1 potassium channel toxin BgK [14]), *m*/*z* 5069.9 from Bg 26.91a, *m*/*z* 5072.9 from Bg 26.91b (type 1 sodium channel toxins BgII and BgIII [52], respectively), *m*/*z* 4593.5 from Bg 30.66b (U-AITX-Bg1a), *m*/*z* 4589.0 from Bg 32.67 (U-AITX-Bg1b), and *m*/*z* 4685.1 from Bg 34.22 (U-AITX-Bg1d).

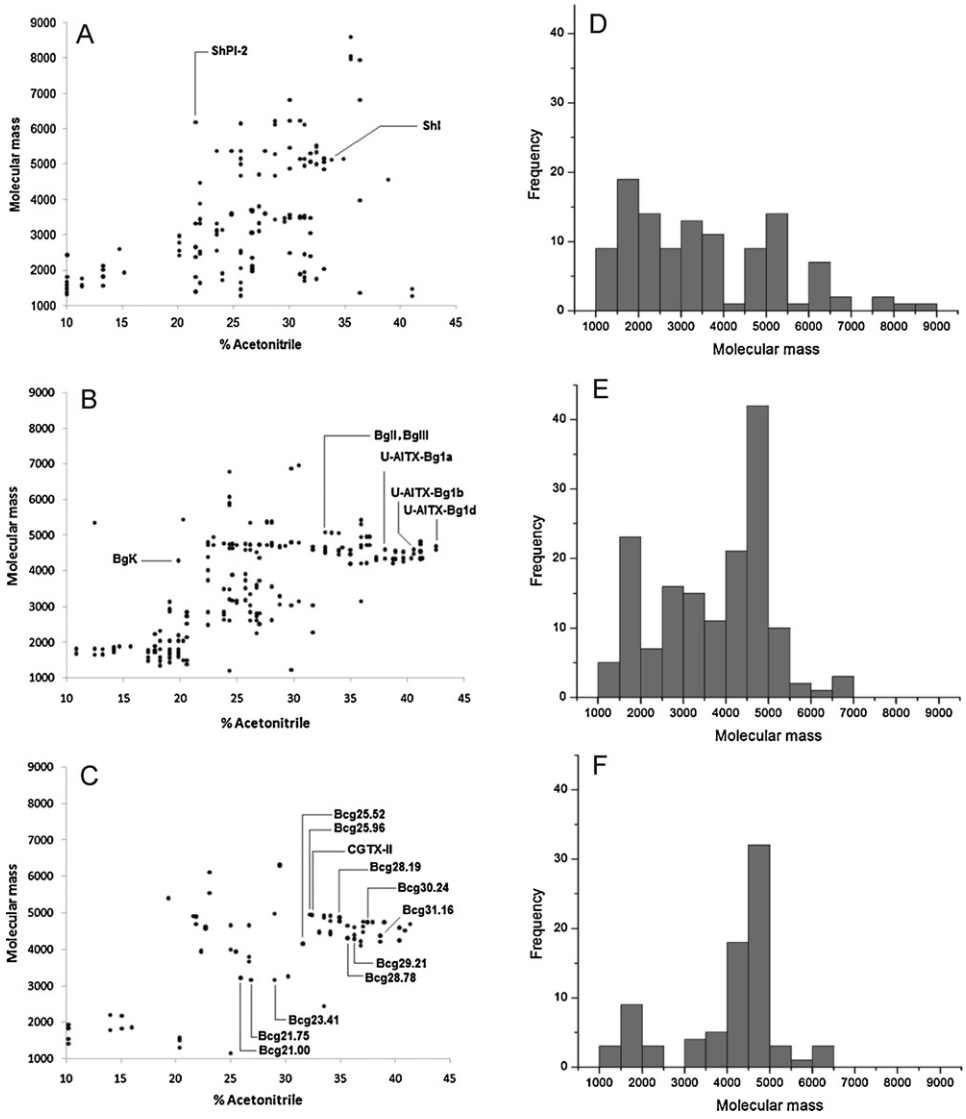

Fig. 3. Peptide maps and molecular mass distributions. *Left side*: Molecular mass vs. %ACN (hydrophobicity) map of sea anemone exudates. Previously reported toxins as well as the new APETx-like peptides are signalized. (A) *Stichodactyla helianthus*: protease inhibitor ShPI-2 [22] and the type 2 sodium channel toxin ShI [43]; (B) *Bunodosoma granulifera*: type 1 potassium channel toxin BgK [14], type 1 sodium channel toxins BgII and BgIII [52] and the new peptides U-AITX-Bg1a, U-AITX-Bg1b, U-AITX-Bg1d; and (C) *Bunodosoma cangicum*: structurally novel peptides Bcg 21.00, Bcg 21.75 and Bcg 23.41 [85], APETx-like peptides Bcg 25.52, Bcg 28.78, Bcg 29.21 and Bcg 31.16 [85], and type 1 sodium channel toxins Bcg 25.96, CGTX-II [84], Bcg 28.19, Bcg 30.24 [85]. *Right side*: Histograms of molecular mass vs. frequency: (D) *Stichodactyla helianthus*, (E) *Bunodosoma granulifera*, and (F) *Bunodosoma cangicum*.

named as U-AITX-Bg1a, U-AITX-Bg1b, U-AITX-Bg1c, U-AITX-Bg1d, and U-AITX-Bg1e (nucleotide sequences deposited at the EMBL Nucleotide Sequence Database having the following accession numbers assigned: HE577144, HE577145, HE577146, HE577147 and HE577148, respectively) according to the nomenclature system proposed by King et al. [44]. Their theoretical molecular masses are 4586.3 Da (U-AITX-Bg1b), 4921.6 Da (U-AITX-Bg1c), 4684.4 Da (U-AITX-Bg1d), and 4142.9 Da (U-AITX-Bg1e); some of them match our experimental values determined in fractions Bg 32.67 (4588.0 Da), Bg 34.22 (4684.1 Da). On the other hand U-AITX-Bg1a was not completely sequenced at the N-terminus; nonetheless the multiple sequence alignment (Fig. 4A) suggested that the missing fragment is GT. Accordingly, the molecular mass of U-AITX-Bg1a should be 4593.3 Da which is in good agreement with the molecular mass of Bg 30.66b (4592.5 Da). For more clarity, refer to Figs. 2B and 3B to observe the peaks from RPC18 chromatography corresponding to the mentioned peptides.

We should also stress that on sequence similarity search procedure, a translated nucleotide sequence from *Anthopleura elegantissima* encoding a putative neurotoxin (GenBank ID: gi|193259782) similar to these U-AITX-Bg1a–e peptides was identified [68]. We named it as U-AITX-Ael1a, following the nomenclature proposed by King et al. [44]. Even though its initial Met amino acid in the precursor is not determined, we may assume that its full CDS is as shown in Fig. 4B, based on the similarity in the alignment with the U-AITX-Bg1a–e peptides here reported. Interestingly, the precursors of U-AITX-Ael1a, U-AITX-Bg1b–d are closely related and present the KR cleavage site, as usual for most of the sea anemone neurotoxins. On the other hand, U-AITX-Bg1e precursor is more variable, being nine amino acids longer than the others and presenting the RR cleavage site. This is the first report of full CDS and precursors for this family of sea anemone toxins, and curiously, species from different genera (*Bunodosoma* vs. *Anthopleura*) present similar precursors, an unusual

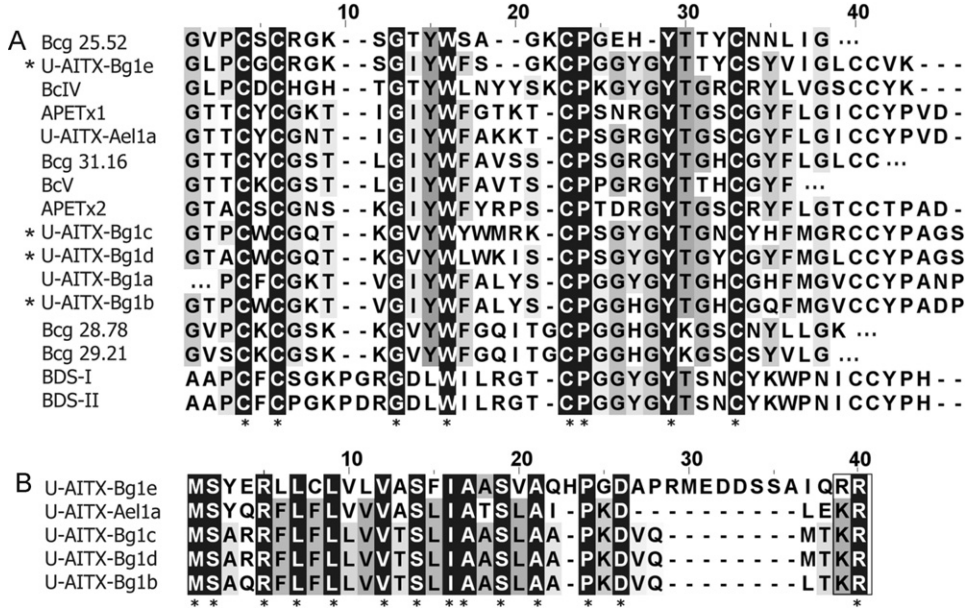

Fig. 4. (A) Multiple sequence alignment of *B. granulifera* mature peptides U-AITX-Bg1 (a–e) and homologues: type 3 potassium channel toxins APETx1 [24], BDS-I and BDS-II [26] from *Anemonia viridis* (formerly *Anemonia sulcata*), the ASIC3 toxin APETx2 [23] and APETx-like peptide U-AITX-Ael1a (deducted from data published in [68]) from the sea anemone *Anthopleura elegantissima*, APETx-like peptide fragments Bcg 25.52, 28.78, 29.21 and 31.16 [85] from *Bunodosoma cangicum*, APETx-like toxins BcIV [64] and BcV (P86470) from *Bunodosoma caissarum*. Asterisks before each toxin name denote peptides which have the complete precursors determined. (B) Multiple sequence alignment of precursor fragments of U-AITX-Bg1 (b–e) and U-AITX-Ael1a. The columns containing entirely conserved positions with identical amino acids are shadowed in black and marked with asterisks, whereas columns shadowed in gray are mainly composed of identical or similar amino acids.

characteristic of sea anemone genes [58–60]. On the contrary, the similarity search against the EST database of *A. viridis* (39,939 ESTs) provided no match to these toxins, revealing that such a category of peptides is not expressed in that species, in agreement to Kozlov and Grishin [45].

3.4. Molecular modeling

Molecular models of U-AITX-Bg1 (a–e), U-AITX-Ael1a and BcIV obtained by the I-Tasser server are represented in Fig. 5. The C-score for each model, as predicted by I-TASSER server were 0.861, 0.814, 0.769, 0.882, 0.570, 0.953 and 0.395 (typically in the range from −5 to 2, higher values signifies a model with a high confidence), respectively. Also, their QMEAN scores and other parameters showed adequate values (data not shown), confirming a good agreement of structures based on APETx1 template and validating our models. Similarly to APETx1 [15] and APETx2 [16], the new APETx-like peptides U-AITX-Bg1 (a, b, d, and e) are composed of a compact core comprising four-stranded β sheets, from which the loop (16–27) and the N- and C-termini emerge. The β sheets sequence obeys (with slight differences) the APETx pattern: residues 3–6 (strand I), 9–14 (strand II), 28–32 (strand III) and 35–39 (strand IV), are connected by a type II β-turn (between strands I and II), a loop (between strands II and III) and a type I β-turn (between strands III and IV). On the other hand, the third strand (28–32) and the type I β-turn, next to this one, are replaced by the loop (16–34) in the U-AITX-Bg1c model. Nevertheless nearly all amino acid residues that compose the basic/aromatic and basic/hydroxyl clusters proposed as interaction surface of APETx2 with ASIC3 [16,25], are conserved in U-AITX-Bg1c (see Fig. 5B). These are R17, R31, F15, Y16, Y32, F33 (basic/aromatic cluster), and S9, K10 (basic/hydroxyl cluster) in APETx2 (see Suppl. Fig. 1B), which are represented by R18, K19, Y15, W16, Y32, F33 (basic/aromatic cluster) and T9, K10 (basic/hydroxyl cluster) in U-AITX-Bg1c. Moreover, although R31 is absent in U-AITX-Bg1c it is worthy of mentioning that R36 is spatially near to R18 and K19; therefore it can be considered as part of the basic/aromatic cluster. Regarding APETx1, it has been proposed an interaction surface comprising the aromatic residues Y5, Y32, and F33, two basic residues, K8 and K18, and three aliphatic amino acids, G7, G31 and L34 [15]. More recently K18 and L34/F33/Y32 have been proposed to be involved in the interaction with hERG channel [86]. Among the new APETx-like peptides, U-AITX-Bg1d is the closest to APETx1 regarding the conservation of all these amino acid residues, which are represented by W5, Y32, F33, K10, K17, G7, G31, and M34 (see Fig. 5B).

Interestingly, as observed also in Fig. 5B, the other peptides U-AITX-Bg1a and 1b do not show positively charged amino acid residues located closely to R17 and R31 positions of APETx2. Those molecules only present a single K8, which is exposed together with F5 and W5 near the N-termini of U-AITX-Bg1a and 1b, respectively. In addition, the electrostatic potentials of such molecules vary a lot, and U-AITX-Bg1a and 1b are the less charged ones. On the contrary, U-AITX-Bg1c and 1e present the most dense positive surfaces. In Suppl. Fig. 1C and D we also depict the electrostatic potentials of APETx1, APETx2, BcIV and the putative new U-AITX-Ael1a. Also, in the same Suppl. Fig. 1B the distribution of positively charged and aromatic residues in U-AITX-Ael1a suggests that such a peptide may represent a "chimera" of contact surfaces of either APETx1 or APETx2.

3.5. Crab bioassay

The crab bioassay is a simple test widely used for the detection of sea anemone toxins [6–8,10,35,37,38,54,73–75,80], mostly acting on sodium channels. Envenomed crabs exhibit a severe paralysis within seconds or few minutes after the injection of a sodium channel toxin. Reactions comprise an initial spastic and tetanic phase, and a later rigid phase followed by death of the crabs [80]. On the other hand, several sea anemone peptides belonging to other classes of toxins have been also discovered, through a careful observation of symptoms provoked on crabs [35,37,38,75].

In the present work we tested all fractions obtained by reversed-phase chromatography. In total, 23 toxic fractions (6 from *S. helianthus* and 17 from *B. granulifera*) were found (Table 1). From

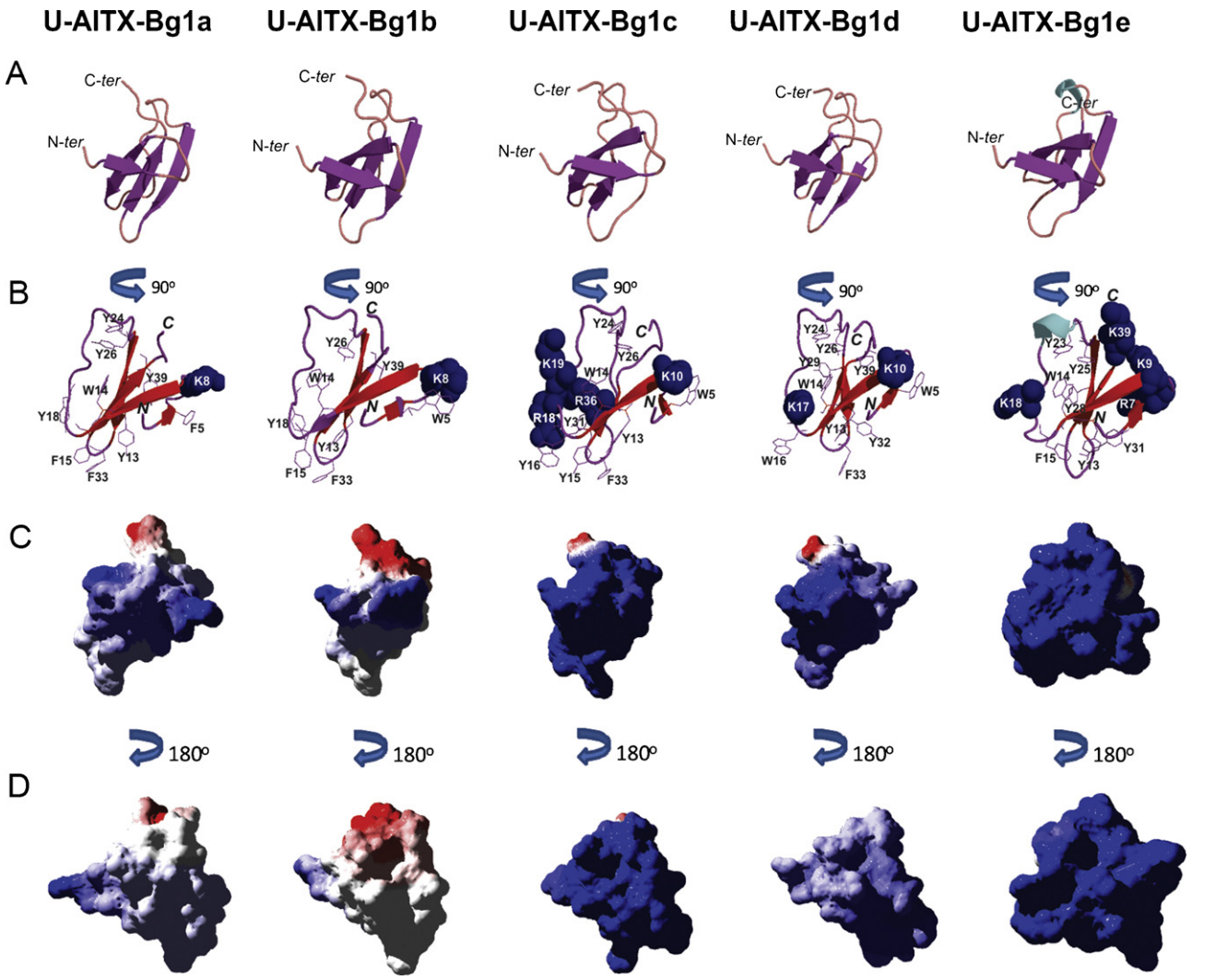

Fig. 5. Molecular modeling of U-AITX-Bg1a–e. (A) Ribbon representation of the lateral view of each toxin. (B) Stereo view of all the positively charged (blue colored spheres) and aromatic (magenta colored lines) amino acids residues side chains of each peptide, rotated 90 degrees to the right of the orientation in panel A. (C) Electrostatic potential of the molecular surface of each peptide, represented in the same orientation as panel A. (D) Electrostatic potential of the molecular surface of each peptide, rotated 180 degrees to the left of the orientation in panel C. Blue colors represent positive charges, as red colors represent negative charges. (For interpretation of the references to color in this figure legend, the reader is referred to the web version of the article.)

these fractions, 15 induced paralysis including spastic and tetanic reactions with different degrees of intensity within seconds to several minutes, resembling the effects provoked by sodium channel toxins. These were Sh 25.05, Sh 26.77, Sh 27.26, Sh 28.12, Bg 10.15, Bg 11.52, Bg 11.95, Bg 12.73, Bg 21.82, Bg 22.34, Bg 23.20, Bg 24.12, Bg 24.55, Bg 26.42 and Bg 26.91. Some particular cases are worthy of highlighting given the early onset of marked paralysis symptoms followed by death of crabs. Fraction Sh 27.26 exhibited a strongly paralyzing effect with lethality to crabs, as expected from the sodium channel toxin ShI [43] which has a similar molecular mass. Small adjacent fractions Sh 26.77 and Sh 28.12 had also similar effects on crabs. Likewise, Bg 26.91, which resulted in Bg 26.91a and Bg 26.91b with molecular masses matching the values of the known sodium channel toxins BgII and BgIII [9,32,71], exhibited lethality to crabs as well as its adjacent fraction Bg 26.42. Other fractions such as Bg 24.12 and Bg 24.55, which predominantly contain smaller peptides (3–3.2 kDa), had similar effects on crabs. Similarly Bg 21.82, a less hydrophobic fraction mainly composed of a 2.8 kDa peptide, was lethal to crabs.

On the contrary the other 8 fractions (Sh 21.48, Sh 21.61, Bg 19.25, Bg 19.68, Bg 19.94, Bg 20.19, Bg 20.79 and Bg 21.57) induced a different paralysis, without any spastic or tetanic reaction. Sh 21.48, Sh 21.61, Bg 19.94, Bg 20.19, Bg 20.79 and Bg 21.57 provoked progressive slowing down of legs movements to ultimately stay motionless, followed by death of the crabs in some cases. Fractions Bg 19.25 and Bg 19.68 provoked, in few minutes, almost total loss of crab legs and pincers, followed by death of animals.

We have noticed that fraction Bg 16.07a, which matched the molecular mass of the type 1 potassium channel toxin BgK, had no effect on crabs. Interestingly, none of the intense last eluting fractions (t_R > 30 min) in the reversed-phase profile of *B. granulifera* (which include APETx-like peptides) was toxic to crabs.

4. Discussion

Sea anemones are well known to contain protein and peptide toxins, mostly grouped into cytolysins and neurotoxins [1,63]. For many years, the bioassay-guided isolations of sea anemone neurotoxins have mainly yielded sodium and potassium channels toxins [39], as well as polypeptides with protease inhibitor activity [63]. However, the recently reported peptidomic and transcriptomic studies demonstrated that the peptide diversity in sea anemones is much more complex [45,85] than previously known, indicating

that new members of known classes of toxins as well as a novel peptide structures, acting on still unknown molecular targets, can be found by using these approaches.

4.1. Comparing peptide diversities of three sea anemone species

In the present study, the neurotoxic fractions of the sea anemones *S. helianthus* and *B. granulifera* were examined by reversed-phase chromatography and mass spectrometry aiming to describe the peptide diversity in terms of molecular mass and retention in reversed-phase chromatography (hydrophobicity). Moreover, a transcriptomic analysis of *B. granulifera* was included to reveal new peptide sequence present in this sea anemone species. This is the first peptidomic and transcriptomic study of the neurotoxic fractions of these sea anemones, and the first report that compares the overall peptide composition of sea anemones species belonging to two distinct families (Stichodactylidae vs. Actiniidae).

We found that the neurotoxic fraction of *B. granulifera* has richer peptide diversity in relation to *S. helianthus*, as judging by the more complex reversed-phase profile and the resulting higher number of separated peptide components (156 vs. 113 peptides) and toxic fractions (17 vs. 6). However a similar study of *B. cangicum* yielded a considerable smaller number of peptide components (81) than *B. granulifera*, despite both sea anemone species belong to the same genus and their chromatographic profiles share a similar complexity and several similarities, therefore such difference does not seem to arise from the use of different mucus extraction methods (immersion in distilled water vs. electrical stimulation).

Our study expanded to 156 the estimated maximal number of peptides in the neurotoxic fraction of sea anemones. We emphasize the term "maximal number" as we showed that venom peptide diversity varies among sea anemone species. Moreover, likewise the previous study [85] we found some apparent venom composition overlaps. Structural studies will confirm whether a single neurotoxic peptide is present in two or more sea anemone species.

Peptide toxins previously isolated and characterized from *S. helianthus* and *B. granulifera* were identified in the present study, with the exception of ShK [14] and ShPI-1 [22]. These toxins seem to be poorly represented in the *S. helianthus* exudate so it was not possible to detect them by mass spectrometry. ShK occurs in very low amounts either in freeze-dried mucus or in whole body extract [14], so its purification included a precipitation step by heating the sample at low pH, prior to the chromatographic protocol. Likewise, the isolation of ShPI-1 comprised a precipitation step (trichloroacetic acid treatment) before the chromatographic separation which included affinity chromatography [22], utilized in many instances as a powerful purification method when the protein of interest is a minor component of a complex mixture [13].

4.2. New APETx-like peptides belonging to the genus Bunodosoma

Our study confirmed the presence of a very distinguishable feature among sea anemone species of the genus *Bunodosoma*, a group of abundant and hydrophobic 4–5 kDa peptides that elute in the last reversed-phase fractions (Figs. 2B and C and 3B and C), so far comprising type 1 sodium channels toxins and APETx-like peptides. The sodium channel toxins are BcIII from *B. caissarum* [55], Bcg 28.19 and Bcg 30.24 from *B. cangicum*, BgII and BgIII from *B. granulifera*. The APETx-like peptides are BcIV from *B. caissarum* [64], Bcg 31.16, Bcg 28.78, Bcg 25.52 and Bcg 29.21 from *B. cangicum* [85] and the new toxins (Fig. 4A) found in our study U-AITX-Bg1a, U-AITX-Bg1b, U-AITX-Bg1d. Two more APETx-like homologous were found, U-AITX-Bg1c and U-AITX-Bg1e, but unfortunately it was not possible to locate them among the peptides found in the examined reversed-phase samples. In previous works it was proposed that APETx-like peptides BcIV, a crab paralyzing toxin, and Bcg 31.16, act on crustacean sodium channels. In contrast, we observed no effect on crabs even at 2000 μg/kg, when tested the last eluting reversed-phase fractions of *B. granulifera*, which include the new APETx-like peptides.

In terms of the possible contact surfaces of these new molecules, Fig. 5B shows that U-AITX-Bg1c and 1d have patches of positively charged and aromatic residues in similar disposition as observed in APETx1 and APETx2 (see Suppl. Fig. 1B for comparison). On the contrary, U-AITX-Bg1a and 1b have only a single K8, which is positioned close to F5 and W5, respectively, forming a putative basic-aromatic dyad. Consequently, these dyads K8/F5 and K8/W5 may represent a possible contact surface of those peptides, which we suggest may dock onto their pharmacological targets in different spatial orientation than the other U-AITX-Bg1 peptides.

In terms of the electrostatic potential of this family of peptides, we observe a great variety (see Fig. 5C and D). Curiously, both APETx1 and APETx2 present a similar distribution of positive and negative charges in their electrostatic potentials (see Suppl. Fig. 1B), however the slight differences among them result in different orientation of their dipole moments and consequently distinct contact surfaces, as reported [15,16,25]. Thus, we may assume that the putative dipole moments of each individual toxin will vary drastically, and the putative contact surfaces of each peptide will be also variable. Anyway, only screening of each individual peptide toward ion channels or receptors may clarify their exact targets and the role of specific residues. In addition we can clearly observe strong evidence that APETx-like peptides constitute a very diverse family of abundant toxins in sea anemones belonging to the family Actiniidae. Therefore, new targets of these peptides, as well as new isoforms, await being properly isolated and characterized.

From the genetic point of view, our data are the first to determine the full CDS of these peptides, including their complete precursors. It also suggests that a micro-heterogeneity of precursors (reflecting possibly variable mature toxins in their C-termini) of this group of peptides occurs, by the comparison of U-AITX-Bg1e with the others, U-AITX-Bg1b–d (from *B. granulifera*) and U-AITX-Ael1a (from *A. elegantissima*).

Our results also indicate that the APETx-like peptide family is not present in *S. helianthus*, a species from a different family. Conversely, type 2 sodium channel toxins are so far represented by ShI in *S. helianthus*. Moreover, the presence of type 1 sodium channel toxins (or other type 2 members) should not be discarded since fractions Sh 26.77, Sh 28.12 as well as Bg 26.42 (from *B. granulifera*) exhibited similar chromatographic behavior, molecular masses and effects on crabs, in relation to sodium channel toxins ShI, BgII and BgIII (Table 1).

4.3. Diversity of crab-paralyzing peptide toxins present in S. helianthus and B. granulifera

Besides the known sodium channel toxins ShI (type 2), BgII, BgIII (type 1) and related fractions Sh 26.77, Sh 28.12 and Bg 26.42 found in the present study, other different sodium channel toxins may be present in chromatographic fractions exhibiting similar effects with lethality to crabs. That is the case of Bg 24.12 and Bg 24.55, which are mainly composed of much smaller peptides (3–3.2 kDa) similarly to type 3 sodium channel toxins Da-I, Da-II, Er-I [36] and PaTX [41]. Another lethal fraction inducing similar effects in comparison with sodium channel toxins is Bg 21.82, mainly composed of an even smaller peptide (2832 Da). The classification of a toxic peptide of this size as a smaller member of type 3 sodium channel toxins should be confirmed by sequencing. Up to date known sea anemone toxins with molecular masses below 3 kDa remain unclassified.

A common feature of the sea anemone species *B. granulifera*, *S. helianthus* and *B. cangicum* [85] is the occurrence of a notable

peptide population in the range of 1.5–2 kDa (Fig. 3D–F), especially abundant in *S. helianthus* and *B. granulifera*. Four fractions composed of very small peptides within that molecular mass range exhibited toxicity to crabs: Bg 10.15, Bg 11.52, Bg 11.95 and Bg 12.73 (Table 1). Up to date no peptide toxin of such small size (at the most 18–19 amino acid residues) has been characterized from sea anemones, therefore these new peptides found in our study are likely to belong to a new class of toxins.

In contrast to the above mentioned toxins we have found several fractions that exhibited a very different paralysis pattern from typical effects provoked by sodium channels toxins. Toxic fractions Sh 21.48, Sh 21.61, Bg 19.94, Bg 20.19, Bg 20.79 and Bg 21.57, which are closely related by their similar RPC18 retention times and effects on crabs, also share the presence of 3–4 kDa peptides (being dominant in Sh 21.48 and Sh 21.61). Most of their toxic components seem to be members of the same family, different from sodium channel toxins. Interestingly, a group of toxins with similar chromatographic behavior and molecular masses were isolated from *B. cangicum* [85] and partially sequenced. Due to the lack of sequence identity with other sea anemone toxins, Bcg 21.00 (3215. 2 Da), Bcg 21.75 (3181 Da) and Bcg 23.41 (3176.4) from *B. cangicum* were grouped into a novel class of peptides. Other sea anemone toxins with molecular masses in the range of 3–4 kDa comprise some type 1 potassium channel toxins and also several unclassified toxins. However, the fraction (Bg 16.07) identified as BgK (type 1 K^+ channel toxin) eluted much earlier than toxins in analysis and had no effect on crabs. These facts suggest that the 3–4 kDa peptides present in Sh 21.48, Sh 21.61, Bg 19.94, Bg 20.19, Bg 20.79 and Bg 21.57 may be new members of the unclassified group of sea anemone toxins previously discovered [85]. Nevertheless, given that the targets on which these toxins exert their effect are still unknown, smaller or larger peptides more represented in some of these fractions might also account for the observed atypical paralyzing effect.

Lastly, toxic fractions Bg 19.68 and Bg 19.25, predominantly composed of 2.6 and 4.8 kDa peptides, provoked a mutilating effect followed by death of crabs. A more exhaustive analysis will reveal whether the peptide toxins implicated in this atypical effect belong to a new class of sea anemone peptides.

5. Conclusions

Applications of peptidomic/peptidomic and transcriptomic to sea anemone venom studies are just starting, whereas other animal venoms have been more extensively explored. In the present work, the neurotoxic fractions of the sea anemones *B. granulifera* and *S. helianthus* were fingerprinted in terms of molecular masses and hydrophobicity. Our study predicted a higher number of peptides than any other study of sea anemones. Moreover we found that type 1 sodium channel toxins and APETx-like peptides constitute the most distinguishable feature of so far studied sea anemone species belonging to *Bunodosoma*, as they are the most abundant and hydrophobic peptides in the neurotoxic fractions of these sea anemones. We found a variety of crab-paralyzing peptides in both sea anemones; although none of them was sequenced, we expect that the smallest ones (<2000 Da) constitute a new family of toxic peptides, given that no crab-paralyzing peptide toxin of such small size has been previously reported.

Acknowledgements

This study was mainly supported by the project CNPq-CITMA 490194/2007-9 (Brazil), a post-doctoral fellowship to AJZ (FAPESP – 07/56525-3), FAPEMIG, INCTTOX, CAPES and CNPq (AMCP and MEL) and the grants from the Science and Technology Development Fund of Macau SAR (Ref. No. 058/2009) and Research Committee, University of Macau (Ref. No. UL017/09-Y1).

We are very grateful to divers José Ramón García and José Ramón Guerra (Cebimar, Cuba) for collecting the sea anemone specimens, Maylin Díaz and Estrella Cuquerella (Cebimar, Cuba) for their assistance in the extraction of sea anemone secretion, Dr. Karla K. Florenço Ferraz (UFMG, Brazil) and Dr. Daniel Moreira dos Santos (UFMG, Brazil) for the molecular masses measurements. A.A. Rodriguez specially thanks Dr. Peter Højrup (Lighthouse data, Denmark) for a copy of the software GPMAW 9.0, and the financial support of the International Foundation for Science (travel grant and research grants F/4082-1, F/4082-2) and the Third World Academy of Sciences (Fellowship for research and advanced training application, and Research grant 06344-2007). None of these organizations were involved in any of the following activities: study design, collection, analysis and interpretation of data, writing of neither the report nor the decision to submit the paper for publication.

Appendix A. Supplementary data

Supplementary data associated with this article can be found, in the online version, at doi:10.1016/j.peptides.2011.10.011.

References

[1] Anderluh G, Macek P. Cytolytic peptide and protein toxins from sea anemones (Anthozoa: Actiniaria). Toxicon 2002;40:111–24.
[2] Aneiros A, Garcia I, Martinez JR, Harvey AL, Anderson AJ, Marshall DL, et al. A potassium channel toxin from the secretion of the sea anemone *Bunodosoma granulifera*. Isolation, amino acid sequence and biological activity. Biochim Biophys Acta 1993;1157:86–92.
[3] Arnold K, Bordoli L, Kopp J, Schwede T. The SWISS-MODEL workspace: a web-based environment for protein structure homology modelling. Bioinformatics 2006;22:195–201.
[4] Benkert P, Biasini M, Schwede T. Toward the estimation of the absolute quality of individual protein structure models. Bioinformatics 2011;27:343–50.
[5] Benkert P, Schwede T, Tosatto SC. QMEANclust: estimation of protein model quality by combining a composite scoring function with structural density information. BMC Struct Biol 2009;9:35.
[6] Beress L, Beress R. Purification of three polypeptides with neuro- and cardiotoxic activity from the sea anemone *Anemonia sulcata*. Toxicon 1975;13:359–67.
[7] Béress L, Béress R. Reinigung zweier krabbenlähmender Toxine aus der Seeanemone *Anemonia sulcata*. Kiel Meeresforsch 1971;27:117–27.
[8] Beress R, Beress L, Wunderer G. Purification and characterisation of four polypeptides with neurotoxic activity from *Condylactis aurantiaca*. Hoppe Seylers Z Physiol Chem 1976;357:409–14.
[9] Bosmans F, Aneiros A, Tytgat J. The sea anemone *Bunodosoma granulifera* contains surprisingly efficacious and potent insect-selective toxins. FEBS Lett 2002;532:131–4.
[10] Bruhn T, Schaller C, Schulze C, Sanchez-Rodriguez J, Dannmeier C, Ravens U, et al. Isolation and characterisation of five neurotoxic and cardiotoxic polypeptides from the sea anemone *Anthopleura elegantissima*. Toxicon 2001;39:693–702.
[11] Calvete JJ, Fasoli E, Sanz L, Boschetti E, Righetti PG. Exploring the venom proteome of the western diamondback rattlesnake, *Crotalus atrox*, via snake venomics and combinatorial peptide ligand library approaches. J Proteome Res 2009;8:3055–67.
[12] Calvete JJ, Sanz L, Cid P, de la Torre P, Flores-Diaz M, Dos Santos MC, et al. Snake venomics of the Central American rattlesnake *Crotalus simus* and the South American *Crotalus durissus* complex points to neurotoxicity as an adaptive paedomorphic trend along Crotalus dispersal in South America. J Proteome Res 2010;9:528–44.
[13] Carlsson J, Janson J-C, Sparrman M. Affinity chromatography. In: Janson J-C, Rydén L, editors. Protein purification principles, high resolution methods and applications. 2nd ed. New York: John Wiley & Sons; 1998.
[14] Castaneda O, Sotolongo V, Amor AM, Stocklin R, Anderson AJ, Harvey AL, et al. Characterization of a potassium channel toxin from the Caribbean Sea anemone *Stichodactyla helianthus*. Toxicon 1995;33:603–13.
[15] Chagot B, Diochot S, Pimentel C, Lazdunski M, Darbon H. Solution structure of APETx1 from the sea anemone *Anthopleura elegantissima*: a new fold for an HERG toxin. Proteins 2005;59:380–6.
[16] Chagot B, Escoubas P, Diochot S, Bernard C, Lazdunski M, Darbon H. Solution structure of APETx2, a specific peptide inhibitor of ASIC3 proton-gated channels. Protein Sci 2005;14:2003–10.
[17] Conlon JM, Coquet L, Leprince J, Jouenne T, Vaudry H, Kolodziejek J, et al. Peptidomic analysis of skin secretions from *Rana heckscheri* and *Rana okaloosae*

provides insight into phylogenetic relationships among frogs of the Aquarana species group. Regul Pept 2007;138:87–93.
[18] Cotton J, Crest M, Bouet F, Alessandri N, Gola M, Forest E, et al. A potassium-channel toxin from the sea anemone *Bunodosoma granulifera*, an inhibitor for Kv1 channels. Revision of the amino acid sequence, disulfide-bridge assignment, chemical synthesis, and biological activity. Eur J Biochem 1997;244:192–202.
[19] Davis J, Jones A, Lewis RJ. Remarkable inter- and intra-species complexity of conotoxins revealed by LC/MS. Peptides 2009;30:1222–7.
[20] de Graaf DC, Aerts M, Danneels E, Devreese B. Bee, wasp and ant venomics pave the way for a component-resolved diagnosis of sting allergy. J Proteomics 2009;72:145–54.
[21] Delfin J, Gonzalez Y, Diaz J, Chavez M. Proteinase inhibitor from *Stichodactyla helianthus*: purification, characterization and immobilization. Arch Med Res 1994;25:199–204.
[22] Delfin J, Martinez I, Antuch W, Morera V, Gonzalez Y, Rodriguez R, et al. Purification, characterization and immobilization of proteinase inhibitors from *Stichodactyla helianthus*. Toxicon 1996;34:1367–76.
[23] Diochot S, Baron A, Rash LD, Deval E, Escoubas P, Scarzello S, et al. A new sea anemone peptide, APETx2, inhibits ASIC3, a major acid-sensitive channel in sensory neurons. EMBO J 2004;23:1516–25.
[24] Diochot S, Loret E, Bruhn T, Beress L, Lazdunski M. APETx1, a new toxin from the sea anemone *Anthopleura elegantissima*, blocks voltage-gated human ether-a-go-go-related gene potassium channels. Mol Pharmacol 2003;64:59–69.
[25] Diochot S, Salinas M, Baron A, Escoubas P, Lazdunski M. Peptides inhibitors of acid-sensing ion channels. Toxicon 2007;49:271–84.
[26] Diochot S, Schweitz H, Beress L, Lazdunski M. Sea anemone peptides with a specific blocking activity against the fast inactivating potassium channel Kv3.4. J Biol Chem 1998;273:6744–9.
[27] Escoubas P, Celerier ML, Nakajima T. High-performance liquid chromatography matrix-assisted laser desorption/ionization time-of-flight mass spectrometry peptide fingerprinting of tarantula venoms in the genus Brachypelma: chemotaxonomic and biochemical applications. Rapid Commun Mass Spectrom 1997;11:1891–9.
[28] Fernandez J, Lomonte B, Sanz L, Angulo Y, Gutierrez JM, Calvete JJ. Snake venomics of Bothriechis nigroviridis reveals extreme variability among palm pitviper venoms: different evolutionary solutions for the same trophic purpose. J Proteome Res 2010;9:4234–41.
[29] Fry BG, Wickramaratna JC, Hodgson WC, Alewood PF, Kini RM, Ho H, et al. Electrospray liquid chromatography/mass spectrometry fingerprinting of Acanthophis (death adder) venoms: taxonomic and toxinological implications. Rapid Commun Mass Spectrom 2002;16:600–8.
[30] Garateix A, Flores A, Garcia-Andrade JM, Palmero A, Aneiros A, Vega R, et al. Antagonism of glutamate receptors by a chromatographic fraction from the exudate of the sea anemone *Phyllactis flosculifera*. Toxicon 1996;34:443–50.
[31] Georgieva D, Ohler M, Seifert J, von Bergen M, Arni RK, Genov N, et al. Snake venomic of *Crotalus durissus* terrificus – correlation with pharmacological activities. J Proteome Res 2010;9:2302–16.
[32] Goudet C, Ferrer T, Galan L, Artiles A, Batista CF, Possani LD, et al. Characterization of two *Bunodosoma granulifera* toxins active on cardiac sodium channels. Br J Pharmacol 2001;134:1195–206.
[33] Guex N, Peitsch MC. SWISS-MODEL and the Swiss-PdbViewer: an environment for comparative protein modeling. Electrophoresis 1997;18:2714–23.
[34] Gutierrez JM, Lomonte B, Leon G, Alape-Giron A, Flores-Diaz M, Sanz L, et al. Snake venomics and antivenomics: proteomic tools in the design and control of antivenoms for the treatment of snakebite envenoming. J Proteomics 2009;72:165–82.
[35] Honma T, Hasegawa Y, Ishida M, Nagai H, Nagashima Y, Shiomi K. Isolation and molecular cloning of novel peptide toxins from the sea anemone *Antheopsis maculata*. Toxicon 2005;45:33–41.
[36] Honma T, Iso T, Ishida M, Nagashima Y, Shiomi K. Occurrence of type 3 sodium channel peptide toxins in two species of sea anemones (*Dofleinia armata* and *Entacmaea ramsayi*). Toxicon 2003;41:637–9.
[37] Honma T, Kawahata S, Ishida M, Nagai H, Nagashima Y, Shiomi K. Novel peptide toxins from the sea anemone *Stichodactyla haddoni*. Peptides 2008;29:536–44.
[38] Honma T, Minagawa S, Nagai H, Ishida M, Nagashima Y, Shiomi K. Novel peptide toxins from acrorhagi, aggressive organs of the sea anemone *Actinia equina*. Toxicon 2005;46:768–74.
[39] Honma T, Shiomi K. Peptide toxins in sea anemones: structural and functional aspects. Mar Biotechnol 2006;8:1–10.
[40] Hutchinson EG, Thornton JM. PROMOTIF – a program to identify and analyze structural motifs in proteins. Protein Sci 1996;5:212–20.
[41] Ishikawa Y, Onodera K, Takeuchi A. Purification and effect of the neurotoxin from the sea anemone *Parasicyonis actinostoloides*. J Neurochem 1979;33:69–73.
[42] Kabsch W, Sander C. Dictionary of protein secondary structure: pattern recognition of hydrogen-bonded and geometrical features. Biopolymers 1983;22:2577–637.
[43] Kem WR, Parten B, Pennington MW, Price DA, Dunn BM. Isolation, characterization, and amino acid sequence of a polypeptide neurotoxin occurring in the sea anemone *Stichodactyla helianthus*. Biochemistry 1989;28:3483–9.
[44] King GF, Gentz MC, Escoubas P, Nicholson GM. A rational nomenclature for naming peptide toxins from spiders and other venomous animals. Toxicon 2008;52:264–76.
[45] Kozlov S, Grishin E. The mining of toxin-like polypeptides from EST database by single residue distribution analysis. BMC Genomics 2011;12:88.
[46] Lagos P, Duran R, Cervenansky C, Freitas JC, Silveira R. Identification of hemolytic and neuroactive fractions in the venom of the sea anemone *Bunodosoma cangicum*. Braz J Med Biol Res 2001;34:895–902.
[47] Lanio ME, Morera V, Alvarez C, Tejuca M, Gomez T, Pazos F, et al. Purification and characterization of two hemolysins from *Stichodactyla helianthus*. Toxicon 2001;39:187–94.
[48] Larkin MA, Blackshields G, Brown NP, Chenna R, McGettigan PA, McWilliam H, et al. Clustal W and Clustal X version 2.0. Bioinformatics 2007;23:2947–8.
[49] Li H, Ruan J, Durbin R. Mapping short DNA sequencing reads and calling variants using mapping quality scores. Genome Res 2008;18:1851–8.
[50] Liang S. Proteome and peptidome profiling of spider venoms. Expert Rev Proteomics 2008;5:731–46.
[51] Liao Z, Cao J, Li S, Yan X, Hu W, He Q, et al. Proteomic and peptidomic analysis of the venom from Chinese tarantula *Chilobrachys jingzhao*. Proteomics 2007;7:1892–907.
[52] Loret EP, del Valle RM, Mansuelle P, Sampieri F, Rochat H. Positively charged amino acid residues located similarly in sea anemone and scorpion toxins. J Biol Chem 1994;269:16785–8.
[53] Ma Y, Zhao R, He Y, Li S, Liu J, Wu Y, et al. Transcriptome analysis of the venom gland of the scorpion *Scorpiops jendeki*: implication for the evolution of the scorpion venom arsenal. BMC Genomics 2009;10:290.
[54] Maeda M, Honma T, Shiomi K. Isolation and cDNA cloning of type 2 sodium channel peptide toxins from three species of sea anemones (*Cryptodendrum adhaesivum*, *Heterodactyla hemprichii* and *Thalassianthus aster*) belonging to the family Thalassianthidae. Comp Biochem Physiol B Biochem Mol Biol 2010;157:389–93.
[55] Malpezzi EL, de Freitas JC, Muramoto K, Kamiya H. Characterization of peptides in sea anemone venom collected by a novel procedure. Toxicon 1993;31:853–64.
[56] Melo F, Feytmans E. Assessing protein structures with a non-local atomic interaction energy. J Mol Biol 1998;277:1141–52.
[57] Meneses EP, Villa-Hernández O, Hernández-Orihuela L, Castro-Franco R, Pando V, Aguilar MB, et al. Peptidomic analysis of the skin secretions of the frog *Pachymedusa dacnicolor*. Amino Acids 2010;40:113–22.
[58] Moran Y, Gordon D, Gurevitz M. Sea anemone toxins affecting voltage-gated sodium channels – molecular and evolutionary features. Toxicon 2009;54:1089–101.
[59] Moran Y, Weinberger H, Lazarus N, Gur M, Kahn R, Gordon D, et al. Fusion and retrotransposition events in the evolution of the sea anemone *Anemonia viridis* neurotoxin genes. J Mol Evol 2009;69:115–24.
[60] Moran Y, Weinberger H, Sullivan JC, Reitzel AM, Finnerty JR, Gurevitz M. Concerted evolution of sea anemone neurotoxin genes is revealed through analysis of the *Nematostella vectensis* genome. Mol Biol Evol 2008;25:737–47.
[61] Neiva M, Arraes FB, de Souza JV, Radis-Baptista G, Prieto da Silva AR, Walter ME, et al. Transcriptome analysis of the Amazonian viper *Bothrops atrox* venom gland using expressed sequence tags (ESTs). Toxicon 2009;53:427–36.
[62] Nunez V, Cid P, Sanz L, De La Torre P, Angulo Y, Lomonte B, et al. Snake venomics and antivenomics of *Bothrops atrox* venoms from Colombia and the Amazon regions of Brazil, Peru and Ecuador suggest the occurrence of geographic variation of venom phenotype by a trend towards paedomorphism. J Proteomics 2009;73:57–78.
[63] Oliveira JS, Fuentes-Silva D, Zaharenko AJ. Sea anemone peptides. Biological activities, structure–function relationships and phylogenetic aspects. In: de Lima ME, Pimenta AM, Martin-Eauclaire MF, Zingali RB, Rochat H, editors. Animal toxins: state of the art perspective in health and biotechnology. 1st ed. Belo Horizonte: Editora UFMG; 2009.
[64] Oliveira JS, Zaharenko AJ, Ferreira Jr WA, Konno K, Shida CS, Richardson M, et al. BcIV, a new paralyzing peptide obtained from the venom of the sea anemone *Bunodosoma caissarum*. A comparison with the Na+ channel toxin BcIII. Biochim Biophys Acta 2006;1764:1592–600.
[65] Pearson WR. Rapid and sensitive sequence comparison with FASTP and FASTA. Methods Enzymol 1990;183:63–98.
[66] Peri S, Steen H, Pandey A. GPMAW – a software tool for analyzing proteins and peptides. Trends Biochem Sci 2001;26:687–9.
[67] Rates B, Ferraz KK, Borges MH, Richardson M, De Lima ME, Pimenta AM. Tityus serrulatus venom peptidomics: assessing venom peptide diversity. Toxicon 2008;52:611–8.
[68] Richier S, Rodriguez-Lanetty M, Schnitzler CE, Weis VM. Response of the symbiotic cnidarian *Anthopleura elegantissima* transcriptome to temperature and UV increase. Comp Biochem Physiol D Genomics Proteomics 2008;3:283–9.
[69] Risch M, Georgieva D, von Bergen M, Jehmlich N, Genov N, Arni RK, et al. Snake venomics of the Siamese Russell's viper (*Daboia russelli siamensis*) – relation to pharmacological activities. J Proteomics 2009;72:256–69.
[70] Roy A, Kucukural A, Zhang Y. I-TASSER: a unified platform for automated protein structure and function prediction. Nat Protoc 2010;5:725–38.
[71] Salceda E, Garateix A, Soto E. The sea anemone toxins BgII and BgIII prolong the inactivation time course of the tetrodotoxin-sensitive sodium current in rat dorsal root ganglion neurons. J Pharmacol Exp Ther 2002;303:1067–74.
[72] Salinas EM, Cebada J, Valdes A, Garateix A, Aneiros A, Alvarez JL. Effects of a toxin from the mucus of the Caribbean sea anemone (*Bunodosoma granulifera*) on the ionic currents of single ventricular mammalian cardiomyocytes. Toxicon 1997;35:1699–709.
[73] Schweitz H, Bidard JN, Frelin C, Pauron D, Vijverberg HP, Mahasneh DM, et al. Purification, sequence, and pharmacological properties of sea anemone toxins from *Radianthus paumotensis*. A new class of sea anemone toxins acting on the sodium channel. Biochemistry 1985;24:3554–61.

[74] Schweitz H, Vincent JP, Barhanin J, Frelin C, Linden G, Hugues M, et al. Purification and pharmacological properties of eight sea anemone toxins from *Anemonia sulcata*, *Anthopleura xanthogrammica*, *Stoichactis giganteus*, and *Actinodendron plumosum*. Biochemistry 1981;20:5245–52.
[75] Shiomi K, Honma T, Ide M, Nagashima Y, Ishida M, Chino M. An epidermal growth factor-like toxin and two sodium channel toxins from the sea anemone *Stichodactyla gigantea*. Toxicon 2003;41:229–36.
[76] Shiomi K, Qian WH, Lin XY, Shimakura K, Nagashima Y, Ishida M. Novel polypeptide toxins with crab lethality from the sea anemone *Anemonia erythraea*. Biochim Biophys Acta 1997;1335:191–8.
[77] Smith PK, Krohn RI, Hermanson GT, Mallia AK, Gartner FH, Provenzano MD, et al. Measurement of protein using bicinchoninic acid. Anal Biochem 1985;150:76–85.
[78] Snyder LR, Dolan JW. Gradient elution fundamentals. In: Snyder LR, Dolan JW, editors. High-performance gradient elution: the practical application of the linear-solvent-strength model. Hoboken, NJ: John Wiley & Sons, Inc.; 2007. p. 23–73.
[79] Songping L. Protocols for peptidomic analysis of spider venoms. In: Soloviev M, editor. Peptidomics: methods and protocols. New York: Humana Press; 2010. p. 75–85.
[80] Ständker L, Beress L, Garateix A, Christ T, Ravens U, Salceda E, et al. A new toxin from the sea anemone *Condylactis gigantea* with effect on sodium channel inactivation. Toxicon 2006;48:211–20.
[81] Tang X, Zhang Y, Hu W, Xu D, Tao H, Yang X, et al. Molecular diversification of peptide toxins from the tarantula *Haplopelma hainanum* (*Ornithoctonus hainana*) venom based on transcriptomic, peptidomic, and genomic analyses. J Proteome Res 2010;9:2550–64.
[82] Vassilevski AA, Kozlov SA, Egorov TA, Grishin EV. Purification and characterization of biologically active peptides from spider venoms. In: Soloviev M, editor. Peptidomics: methods and protocols. New York: Humana Press; 2010. p. 87–100.
[83] Waterhouse AM, Procter JB, Martin DM, Clamp M, Barton GJ. Jalview Version 2 – a multiple sequence alignment editor and analysis workbench. Bioinformatics 2009;25:1189–91.
[84] Zaharenko AJ, Ferreira Jr WA, de Oliveira JS, Konno K, Richardson M, Schiavon E, et al. Revisiting cangitoxin, a sea anemone peptide: purification and characterization of cangitoxins II and III from the venom of *Bunodosoma cangicum*. Toxicon 2008;51:1303–7.
[85] Zaharenko AJ, Ferreira Jr WA, Oliveira JS, Richardson M, Pimenta DC, Konno K, et al. Proteomics of the neurotoxic fraction from the sea anemone *Bunodosoma cangicum* venom: novel peptides belonging to new classes of toxins. Comp Biochem Physiol D Genomics Proteomics 2008;3:219–25.
[86] Zhang M, Liu XS, Diochot S, Lazdunski M, Tseng GN. APETx1 from sea anemone *Anthopleura elegantissima* is a gating modifier peptide toxin of the human ether-a-go-go-related potassium channel. Mol Pharmacol 2007;72:259–68.
[87] Zhang Y. Template-based modeling and free modeling by I-TASSER in CASP7. Proteins 2007;69(Suppl. 8):108–17.
[88] Zhou H, Zhou Y. Distance-scaled, finite ideal-gas reference state improves structure-derived potentials of mean force for structure selection and stability prediction. Protein Sci 2002;11:2714–26.

Glossary

t_D: System dwell time (min).
ϕ: Volume fraction of B solvent in the mobile phase.
t_G: Gradient time (min).
t_M: Column dead time (min), retention time of an unretained peak.
t_R: Retention time (min).
t_{delay}: Gradient delay time (min), corresponding to initial isocratic elution before the start of the gradient.
RPC18: Reversed-phase octadecyl stationary phase.
CDS: Coding sequence.
emPCR: Emulsion PCR.